Communication—Enhancing the Electrochemical Performance of Lithium-Excess Layered Oxide $Li_{1.13}Ni_{0.3}Mn_{0.57}O_2$ via a Facile Nanoscale Surface Modification

Haodong Liu,* Jiajia Huang, Danna Qian, Sunny Hy, Chengcheng Fang, Jian Luo, and Ying Shirley Meng**,z**

Department of NanoEngineering, University of California San Diego, La Jolla, California 92093, USA

In this work, a facile surface modification with nanoscale equilibrium Li_3PO_4-based surface amorphous films (SAFs) has been applied to Lithium-excess layered oxide $Li_{1.13}Ni_{0.3}Mn_{0.57}O_2$, which significantly improves the first cycle coulombic efficiency, rate capability, and cycling stability. The nanoscale surface modification can be easily achieved by ballmilling and isothermal annealing. The optimized surface modified $Li_{1.13}Ni_{0.3}Mn_{0.57}O_2$ is capable of maintaining a high capacity of 201 mAh g^{-1} after 60 cycles at 55°C testing with a rate of 1 C. This work provides a facile and scalable surface modification method to improve electrochemical performance of cathode materials for lithium ion batteries.

The Lithium-excess layered oxides benefit from an extraordinary high reversible capacity (>280 mAh g^{-1}) and is one of the most promising cathode materials for plug-in electric vehicle application.[1–3] However, this high-energy-density material suffers from large irreversible capacity in its first electrochemical cycle when it is charged to high voltages, namely more than 4.6 V. In addition, its rate capability is yet unsatisfactory for high power application. Moreover, the gradual voltage and capacity degradation upon electrochemical cycling, especially at elevated temperature when side reactions related to the interactions with the electrolyte occur more prevalently, represent the most serious technical challenge for this material.[4,5] In the past few years, significant amount of surface modification works have been carried out to protect the surfaces of the Li-excess. Most of the reported surface modifications are performed under solution-based reactions.[6–8] For example, Bian et al. used LiOH and $NH_4H_2PO_4$ to coat Lithium-excess with Li_3PO_4.[7] However, the solution based surface modification adds an additional layer of complexity for preparation of Lithium-excess, which will definitely raise the cost of production. Although Konishi coated high voltage spinel $LiNi_{0.5}Mn_{1.5}O_4$ with uniform Li_3PO_4 via pulsed laser deposition (PLD), this technique requires special equipment, which is difficult to realize for large scale production.[9]

In this work, we modify the surface of Lithium-excess layered oxide $Li_{1.13}Ni_{0.3}Mn_{0.57}O_2$ via simple mixing and calcination to form Li_3PO_4-enriched and nanometer-thick surface amorphous films (SAFs).[10] Our results indicate that the optimized material shows remarkably improved performance.

Experimental

The synthesis of the Li-excess is described in our previous publications.[3,6] The procedure for preparing Li_3PO_4 surface modified $Li_{1.13}Ni_{0.3}Mn_{0.57}O_2$ (LPLNMO) was adapted from work by Huang et al.[10] 0.06 g Li_3PO_4 (Alfa Aesar, 99.99%) and 3 g $Li_{1.13}Ni_{0.3}Mn_{0.57}O_2$ were mixed using a planetary ball mill (PM 100, Retsch). The powder was calcinated at 500°C (LP500), 600°C (LP600), and 700°C (LP700), respectively, for 5 h in air. Electrochemical test, XRD, SEM and HRTEM characterization are described with details in our previous work.[1,6]

Results and Discussion

Results.—Figure 1 shows the SEM images of the LNMO and LPLNMOs. All materials show secondary particles with a wide size distribution below 10 μm; the primary particle size distribution ranges from 50 to 200 nm. There were no dramatic changes to the morphology or particle size after Li_3PO_4 surface modification.

HRTEM is used to identify the Li_3PO_4 coating (SAFs) on LP600. The TEM images show very good layered bulk crystal structure, and amorphous films on the surface of LP600. More than 20 particles are analyzed to examine the amorphous film. As shown in Figure 1i, particles have the amorphous film evenly coated on the surface, with the thickness of ~2 nm. While the majority of particles exhibit uniform coatings, there are some particles that still show clean surfaces with no indication of surface coatings, as illustrated in Figure 1j.

The XRD of LNMO and LPLNMOs are refined and plotted in Figure 2. The major diffraction peaks of these materials are indexed to the $R\bar{3}m$ space group.[1,11,12] No obvious changes were observed in these peaks after Li_3PO_4 surface modification, suggesting that the layered phase is well retained. The lattice parameters of LNMO are a = 2.8641(3) Å and c = 14.253(2) Å. Both LP500 and LP600 show no change in lattice parameters, however, LP700 demonstrates expanded lattices, which suggests the bulk structure changes under high temperature calcination.

Figures 3a–3d illustrate the first charge/discharge voltage profiles of LNMO and LPLNMOs within the voltage window of 2–4.8 V, at 12.5 mA g^{-1} (C/20). The LNMO delivers a charge capacity of 317 mAh g^{-1}, and a discharge capacity of 223 mAh g^{-1}. A low coulombic efficiency of 70.4% has been observed in LNMO. The LP500 demonstrates similar charge capacity of 319 mAh g^{-1}, but much higher discharge capacity of 261 mAh g^{-1}. Consequently, the coulombic efficiency of LP500 increases to 81.2%. In contrast, the charge capacity of LP600 decreases to 299 mAh g^{-1} while the discharge capacity increases to 258 mAh g^{-1} at the same time. Both factors contribute to a compressed irreversible capacity of 41 mAh g^{-1} leading to the relatively higher coulombic efficiency of 86.3%. Once the calcinations temperature is raised to 700°C, the LP700 exhibits a high irreversible capacity of 110 mAh g^{-1}. Figure 3e compares the capacities of these materials at different discharge rates. Among all the materials, LP600 shows the highest coulombic efficiency and best rate capability.

The long-term cycling performance of LNMO and LPLNMOs were compared, which is represented in Figure 3f. Over the course of 100 cycles, LNMO, LP500, and LP700 suffer from significant capacity fading. According to the XRD results, the bulk structure of LP700 was changed by high temperature calcination which may accelerate the capacity degradation upon cycling. Although the bulk structure of LP500 is retained, the temperature is not high enough to form an effective coating layer on the layered oxides.[10] Both LNMO and LP600 are cycled for extra 50 times. After 150 cycles, the capacity difference between the LNMO and LP600 increases to 49 mAh g^{-1}, which is larger than 36 mAh g^{-1} of the first cycle.

*Electrochemical Society Student Member.
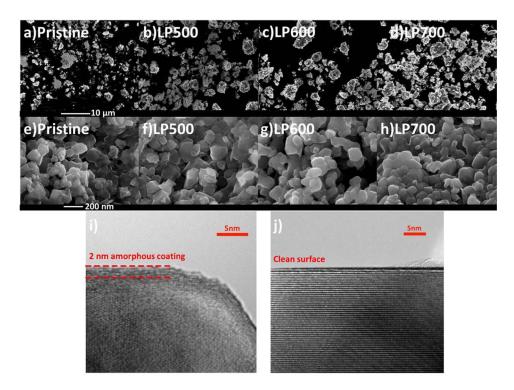**Electrochemical Society Member.
zE-mail: shirleymeng@ucsd.edu

Figure 1. SEM images: (a)–(h). TEM images of LP600: (i) particles with coating and (j) particles that were surface modified but still were not coated.

Both LNMO and LP600 are cycled at 55°C within the voltage window of 2–4.8 V, at 250 mA g^{-1}. Figure 4a compares their first charge/discharge voltage profiles. Both materials show larger charge/discharge capacities than their low current testing values at room temperature, which is due to the higher lithium activity at elevated temperature.[10] An obvious elongated slope (∼ 218 mAh g^{-1}) appears in LNMO, which indicates the reactions between electrode and electrolyte happens below 4.4 V at 55°C. After the Li$_3$PO$_4$ surface modification, the charge capacity decreases from 390 to 332 mAh g^{-1} while the discharge capacity increases from 246 to 271 mAh g^{-1}, respectively. The corresponding coulombic efficiency escalates from 63.1% to 81.6%.

The charge/discharge capacities of both materials are compared in Figure 4b. Large irreversible capacities exist in each cycle of LNMO,
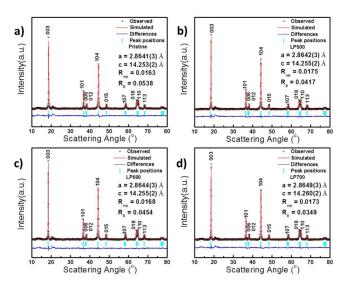
while the LP600 only exhibits irreversible capacity in its first cycle. LP600 delivers 201 mAh g^{-1} with an enhanced capacity retention of 74.2% after 60 cycles. As a comparison, LNMO only shows 41% capacity of its first cycle.
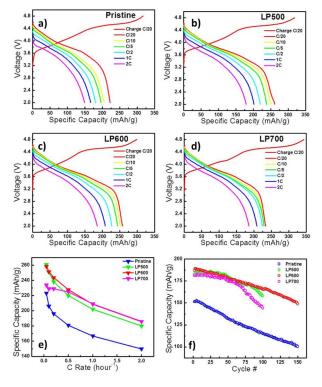

Figure 3. Comparison of electrochemical performances between LNMO and LPLNMOs: (a)–(d) voltage profiles under different current density; (e) discharge capacity under different current density; and (f) comparison of capacity upon cycling, the voltage range is 2.0–4.8 V at 1 C = 250 mA g^{-1}.

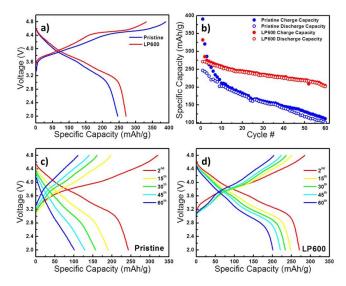**Figure 2.** XRD patterns and refinements of (a) LNMO, (b) LP500, (c) LP600, and (d) LP700.

Figure 4. Comparison of electrochemical performances between LNMO and LP600 at 55°C: (a) first cycle voltage profile; (b) comparison of capacity over the course of 60 cycles; (c) and (d) voltage profiles at different cycles. The voltage range is 2.0–4.8 V at 1 C = 250 mA g^{-1}.

General discussions.—LP600 delivers a high coulombic efficiency of 86.4% in its first cycle. Both suppressed irreversible lattice oxygen loss and reduced undesired side reactions with electrolyte lead to lower charge capacity, which is indicated by the shorter charge plateau. As a consequence, LP600 gets a better electrode/electrolyte interphase, which facilitates the lithium transports during discharge and following cycles. The high temperature tests are designed to verify this hypothesis. In Figures 4c–4d, the LNMO demonstrates large discharge voltage slippage, which indicates the rapid growth of cathode electrolyte interphase (CEI) on the surface of LNMO.[4–6] This undesired CEI traps or slows down the lithium diffusion, thus causing serious capacity and voltage degradation in LNMO. In the case of LP600, the CEI is mitigated by the Li$_3$PO$_4$ coating layer by reducing direct contact between the electrode and electrolyte. In addition, the Li$_3$PO$_4$ coating layer protects the electrode from etching by acidic species in the electrolyte.[8,13] Moreover, the surface reconstruction of Li-excess may also be alleviated through suppressing the oxygen loss. The Li$_3$PO$_4$ coating improves the voltage stability for Lithium-excess, however, it is suggested that surface modification, bulk substitution, and interphase optimization should work together in order to overcome the voltage fading in Li-excess.

Conclusions

In this work, we applied nanoscale self-regulated Li$_3$PO$_4$-based surface amorphous films to Lithium-excess layered oxide Li$_{1.13}$Ni$_{0.3}$Mn$_{0.57}$O$_2$ via a facile method. The mixture of 2 wt% Li$_3$PO$_4$ and Li$_{1.13}$Ni$_{0.3}$Mn$_{0.57}$O$_2$ annealed at 600°C shows significantly improved coulombic efficiency in first cycle, rate capability, and cycling stability of Li-excess. These improvements are valid even at an elevated temperature. We expect that this scalable method will also work for other high voltage cathode materials for lithium ion batteries.

Acknowledgments

References

1. M. G. Verde, H. D. Liu, K. J. Carroll, L. Baggetto, G. M. Veith, and Y. S. Meng, *Acs Appl Mater Inter*, **6**(21), 18868 (2014).
2. H. Liu, Y. Chen, S. Hy, K. An, S. Venkatachalam, D. Qian, M. Zhang, and Y. S. Meng, *Advanced Energy Materials*, n/a-n/a (2016).
3. H. D. Liu, C. R. Fell, K. An, L. Cai, and Y. S. Meng, *J Power Sources*, **240** 772 (2013).
4. S. Hy, F. Felix, J. Rick, W. N. Su, and B. J. Hwang, *J Am Chem Soc*, **136**(3), 999 (2014).
5. S. Hy, S. Felix, Y. H. Chen, J. Y. Liu, J. Rick, and B. J. Hwang, *J Power Sources*, **256** 324 (2014).
6. H. Liu, D. Qian, M. G. Verde, M. Zhang, L. Baggetto, K. An, Y. Chen, K. J. Carroll, D. Lau, M. Chi, G. M. Veith, and Y. S. Meng, *Acs Appl Mater Inter*, **7**(34), 19189 (2015).
7. X. F. Bian, Q. Fu, X. F. Bie, P. L. Yang, H. L. Qiu, Q. Pang, G. Chen, F. Du, and Y. J. Wei, *Electrochim Acta*, **174** 875 (2015).
8. J. Zheng, M. Gu, J. Xiao, B. J. Polzin, P. Yan, X. Chen, C. Wang, and J.-G. Zhang, *Chem Mater*, **26**(22), 6320 (2014).
9. H. Konishi, K. Suzuki, S. Taminato, K. Kim, Y. M. Zheng, S. Kim, J. Lim, M. Hirayama, J. Y. Son, Y. T. Cui, and R. Kanno, *J Power Sources*, **269** 293 (2014).
10. J. J. Huang and J. Luo, *Phys Chem Chem Phys*, **16**(17), 7786 (2014).
11. H. D. Liu, J. Xu, C. Z. Ma, and Y. S. Meng, *Chem Commun*, **51**(22), 4693 (2015).
12. J. Xu, H. Liu, and Y. S. Meng, *Electrochemistry Communications*, **60** 13 (2015).
13. J. M. Zheng, P. H. Xu, M. Gu, J. Xiao, N. D. Browning, P. F. Yan, C. M. Wang, and J. G. Zhang, *Chem Mater*, **27**(4), 1381 (2015).